Projected changes in the tropical Pacific Ocean of importance to tuna fisheries

Alexandre Ganachaud, Alexander Sen Gupta, Jaclyn Brown, Karen Evans, Christophe Maes, Les Muir, Felicity Graham

Climatic Change - Special Issue on Climate and Ocean Fisheries manuscript No.
(will be inserted by the editor)

Projected changes in the tropical Pacific Ocean of importance to tuna fisheries

DOI 10.1007/s10584-012-0617-z
The final publication is available at www.springerlink.com

Alexandre Ganachaud · Alexander Sen Gupta · Jaclyn N. Brown · Karen Evans · Christophe Maes · Les C. Muir · Felicity S. Graham

Received: 26 January 2012 / Accepted: 9 October 2012

Abstract Future physical and chemical changes to the ocean are likely to significantly affect the distribution and productivity of many marine species. Tuna are of particular importance in the tropical Pacific, as they contribute significantly to the livelihoods, food and economic security of island states. Changes in water properties and circulation will impact on tuna larval dispersal, preferred habitat distributions and the trophic systems that support tuna populations throughout the region. Using recent observations and ocean projections from the CMIP3 and preliminary results from CMIP5 climate models, we document the projected changes to ocean temperature, salinity, stratification and circulation most relevant to distributions of tuna. Under a business-as-usual emission scenario, projections indicate a surface intensified warming in the upper 400 m and a large expansion of the western Pacific Warm Pool, with most surface waters of the central and western equatorial Pacific reaching temperatures warmer than 29°C by 2100. These changes are likely to alter the preferred habitat of tuna, based on present-day thermal tolerances, and in turn the distribution of spawning and foraging grounds. Large-scale shoaling of the mixed layer and increases in stratification are expected to impact nutrient provision to the biologically active layer, with flow-on trophic effects on the micronekton. Several oceanic currents are projected to change, including a strengthened upper equatorial undercurrent, which could modify the supply of bioavailable iron to the eastern Pacific.

Keywords Climate Change · Ocean Circulation · Stratification · Thermocline · Sea Surface Temperature · Warm Pool · Equatorial Upwelling · Tuna · Fisheries · Skipjack · CMIP3 · CMIP5

PACS 92.70.Jw · 92.70.Gt · 92.70.Er · 92.10.Gk

This work was partly funded by ANR project ANR-09-BLAN-0233-01; it is a contribution to the CLIVAR/SPICE. Part of the research was conducted with the support of the Pacific Australia Climate Change Science and Adaptation Program (PACCSAP), a program managed by the Department of Climate Change and Energy Efficiency in collaboration with AusAID, and delivered by the Bureau of Meteorology and the Commonwealth Scientific and Industrial Research Organisation (CSIRO).

A. Ganachaud (corresponding author), C. Maes
Institut de Recherche pour le Développement (IRD), UMR5566, LEGOS, BP A5, Nouméa, New Caledonia
Tel.: +687-260812
UPS (OMP-PCA); LEGOS; Toulouse, France
E-mail: Alexandre.Ganachaud@ird.fr

A. Sen Gupta
University of New South Wales, Sydney Australia

J. N. Brown, K. Evans, L. Muir, F. S. Graham
Wealth from Oceans National Research Flagship, CSIRO Marine and Atmospheric Research, Hobart, Australia

1 Introduction

Tuna harvested from the tropical Pacific Ocean and the ecosystems that support them depend intimately on the oceanic environment. The distribution of these marine predators is linked to the horizontal displacement of water of a suitable temperature, and to vertical changes in the depth of the mixed layer. Areas where currents diverge or converge are also of major importance because they are associated with the thermal fronts, upwelling and eddies which enhance local productivity and, in turn create important foraging areas.

Tuna make up the overwhelming majority of fish harvested in the tropical Pacific Ocean and contribute significantly to the livelihoods, food and economic security of many island nations throughout the region (Bell et al. 2011, chapt. 1). A number of species are of particular importance including: skipjack (*Katsuwonus pelamis*, which comprise more than 60% of the catches in the region), yellowfin (*Thunnus albacares*), bigeye (*Thunnus obesus*) and albacore tuna (*Thunnus alalunga*). The response of these predators to oceanic conditions varies between species and life stage (i.e. larvae, juvenile and adult) and is primarily associated with the physiology of the species and how the species they prey on -the *micronecton*- are distributed. Of the four species, skipjack tuna appear to have the most limited physiology, with adults predominately occurring in waters with a temperature range of $20^\circ - 29^\circ$C and with a dissolved oxygen concentration above $\sim$ 4.0 ml/l. Temperature and oxygen tolerances are generally wider in the other three species with albacore predominantly occurring in cooler waters than yellowfin and bigeye, and bigeye able to tolerate lower dissolved oxygen concentrations than yellowfin and albacore (Bushnell and Brill 1992). Tuna are most sensitive to water temperatures during their larval stages, with thermal tolerances widening as they grow. The distribution of primary production is also important for earlier life stages of tuna and micronekton. This distribution will depend on both the physical and chemical properties of the ocean and in particular, the availability of oceanic nutrients. These are abundant at depths, most often below the biologically-active layer (*euphotic zone*), and the supply to this euphotic zone depends upon oceanic currents and mixing processes.

Five ecological areas will guide our analysis, each with distinct vertical hydrological structure and ecosystems (Figure 1a): the Pacific Equatorial divergence (PEQD) the Pacific Warm Pool (WP), the North Pacific Tropical Gyre (NPTG), the South Pacific Subtropical Gyre (SPSG) and the Archipelagic Deep Basins (ARCH; Longhurst 2006). The time-dependent boundaries between each of these provinces are predominantly associated with the convergence zones of ocean surface currents. Of particular relevance to tuna catches in the western Pacific is the boundary that exists between WP and PEQD, the position of which is influenced by the El Niño Southern Oscillation (ENSO), moving eastward during El Niño and westward during La Niña by thousands of kilometres (Maes et al. 2004). More than 90% of skipjack tuna catches are located within the WP and demonstrate associated shifts in distributions with ENSO (Lehodey et al. 1997, this issue). Any future changes to the WP or to the characteristics of ENSO could therefore have a large influence on the availability of tuna stocks to Pacific island states and to their associated economies.

This paper provides fisheries scientists and managers with information on future projections of the physical properties of the tropical Pacific. We focus on the parameters that are of relevance to tuna, and in particular, skipjack tuna, as this species comprises the greatest proportion of tuna catches throughout this region (Lehodey et al. 1997). We first introduce the climate models used to project the ocean state (Section 2), then examine changes to surface and subsurface temperatures, vertical stratification, major ocean currents and upwelling, as well as issues associated with future projection of ENSO (Section 3). Finally, we describe some of the limitations inherent in those projections and discuss the implications for tuna as a result of the projected physical changes (Section 4).

2 Methods

To examine future changes to the ocean we use output from the third Coupled Model Intercomparison Project (CMIP3), archived by the Program for Climate Model Diagnoses Intercomparison (PCMDI). The CMIP3 repository contains 24 nominally independent models encompassing a broad range of resolutions and a variety of physical parameterizations (Sen Gupta et al. 2009, Table 1). Ocean horizontal resolutions vary from $\frac{1}{4}^\circ$ to 5°. Unless otherwise stated we compare present day conditions from the end of the 20th century (1980-2000) with future projections for 2100 and from the *business as usual* SRESA2 emissions scenario (Nakicenovic et al. 2000). Projections for 2100 are calculated by taking a linear trend in a variable over the full 21st century-unless otherwise stated, to minimize the effect of low frequency variability that can distort the climate change signal. The significance of projected changes is established using a standard t-test. This assumes independence among the models, which may lead to overestimation of the areas where the changes should be considered significant (Pennel and Reichler 2011).

Some climate models exhibit spurious trends, unrelated to external forcing, that may affect the estimated climate change signal. This *drift* is of a different sign, magnitude and spatial distribution in different models and as such has a negligible effect on averages across multiple models (Sen Gupta et al 2012b; Tebaldi and Knutti 2007). As the analysis below generally focusses on the multi-model mean (MMM), we have neglected errors introduced by model drift. However, when considering individual models, drift is likely to be a small additional source of uncertainty.

We have adopted the approach of examining the largest number of models possible for each diagnostic. As such, the number of models used may vary in a given analysis (Online Table S1). Given the importance of ENSO behaviour on tuna, we also include preliminary analysis on the currently available subset of models taking part in CMIP5 when discussing projected changes to interannual variability.

3 Results

3.1 Sea surface temperatures

Under typical conditions, trade winds push the warmest tropical waters to the western side of the Pacific basin, forming the WP, where sea surface temperature (SST) generally exceeds 29°C (Fig.1a). Along the equator and the coast of South America, the prevailing winds cause equatorial and coastal upwelling, respectively, forming the PEQD, a relatively cool tongue of water (SST$<$ 20°C) that extends across the Pacific and meets the eastern edge of the WP. At 10°N, a band of warm water extends across the entire basin, below the intertropical convergence zone (ITCZ). At 10°S, a similar band only extends to 140°W a result of the South Pacific Convergence Zone (SPCZ) being confined to the western Pacific. SST varies seasonally by $\pm 2-3$°C near 25°N/S (e.g., Bell et al. 2011, chapt. 2), but by only ±1°C within 15° of the equator, where instead interannual variability dominates (±2°C, Section 3.5). Over the 1955-2003 period, warming trends of about 0.2° to 1°C have been observed in the western Pacific (Cravatte et al. 2009), thereby increasing the horizontal extent of the WP waters with temperatures greater than 29°C.

The CMIP3 MMM reproduces the observed large-scale temperature field (Fig.1b). However, there is a systematic cold offset, or *bias* in the central and western equatorial Pacific (i.e. the bias is present in almost all the models) with simulated temperatures up to 2°C too low in the MMM, with more extreme biases in individual models (Fig.1c). Conversely, on the eastern boundaries, upwelling is too weak and temperatures too warm.

The projections for 2100 suggest a statistically significant MMM warming that exceeds 2.5°C over large parts of the basin. The physical mechanisms driving the spatial pattern of this warming are reasonably well understood: a projected increase in the south easterly trade winds (south of the equator), leads to a relatively slow warming rate in the southeastern Pacific (Xie et al. 2010) while the enhanced equatorial warming is related in part to a weaker Walker circulation (DiNezio et al. 2009).

The WP region is projected to warm in all models, with the warmest 9 million square km (which correspond to the area of water enclosed by the 29°C isotherm in observations) increasing by $\sim 2.7 \pm 0.4$°C (±0.4° is the standard deviation among the CMIP3 models). This is associated with the eastern edge of the WP (as defined by the 29°C isotherm) moving east by 6000 ± 2000 km (Fig.2a). Projections also show that the warming will be greatest in the cold tongue ($>$ 3°C east of 140°E, Section 4).

It is often more pertinent to define the WP edge by a certain salinity surface (*isohaline*) than an isotherm (i.e. 29°C). This alternative definition better reflects the position of the front generated by strong rainfall in the west and is a better proxy for the convergence zone between WP (or *fresh pool*) and PEQD. The WP surface salinity has decreased substantially over the past 50 years (1955-2003, 0.34 PSU, Cravatte et al. 2009), although the extent to which natural variability has contributed to this is uncertain. While the CMIP3 models also generally simulate a freshening in the WP over this period, the magnitudes of change are considerably smaller. The CMIP3 models generally project further freshening (Online Figure S1) due to increased rainfall over the WP and convergence zones. Projections suggest that the edge of the fresh pool will be displaced eastward by $\sim 500-2000$ km by 2100, much less than the WP (Fig.2a).

3.2 Vertical temperature and salinity structure

Near the equator, WP waters extend to depth of $\sim$ 100 m, overlying a steep thermocline situated between 100 and 250 m (Fig.3a). In PEQD the mixed layer and the thermocline are considerably shallower. Observational data from 1950 to 2008 show that surface warming of the central Pacific has penetrated vertically from 50 m to 100 m at the equator to the top of the thermocline ($>$ 1°C down to 100 m, Fig.3c). Surprisingly, in the western Pacific, water temperatures have actually decreased by up to 2°C through the thermocline depths

($100-150$ m, Fig.3c). It has been suggested that this cooling is related to a weakening of the easterly equatorial winds that through dynamical ocean processes cause an adiabatic lifting of the thermocline (Han et al. 2006). Vecchi et al (2008) note however that the brevity of the data record precludes attributing the changes in the Walker circulation to anthropogenic Global Warming. The depth of the observed warming varies with latitude (Online Figure S2a), reaching 400 to 600 m in the northern hemisphere subtropics (not shown; see Bell et al. 2011, chapt. 3). The subsurface cooling noted in the western equatorial region ($10°$S$-10°$N) is evident between $\sim 100-250$ m. It extends southwards reaching depth exceeding 800 m in the southern hemisphere subtropical gyre (not shown). This enhanced vertical contrast is also observed in the salinity change, with a decrease in the WP and an increase in the thermocline waters below the WP (Durack and Wijffels 2010).

In the equatorial band, projected MMM warming is generally confined within the model mixed layer, reaching $+2.5°$C at 50 m and $\sim +1°$C at 100 m$-$ which is of a similar magnitude to observed trends of the 20th century (Fig.3c, 4a). Poleward of $10°$N/S, the projected warming penetrates to considerably greater depths than at the equator, with a warming of $\sim 1.5°$C at 200 m (Fig.2e, 4c). Below 100 m, and west of about $140°$W, very weak warming or moderate cooling is projected to occur straddling the equator (Fig.3e), at about 160 m and within $10°$N/S. The cooling pattern is also similar to the observed trends and is again consistent with a shoaling of the thermocline driven by a weakening of the equatorial trade winds. Projected salinities also show an enhanced freshening in the WP (Online Figure S1) down to $\sim$50 m (not shown).

3.3 Stratification and mixed layer depth

Stratification, which is associated with the density difference between the surface and the deep oceanic layers, characterizes the stability of the water column, and therefore the potential extent of vertical exchange of properties such as nutrients or oxygen. Its interplay with the mixed layer, the region of homogenized temperature, salinity, oxygen and nutrients that extends from the surface to the mixed layer depth (MLD), has important influences on primary production (Section 4).

The combined effect of the surface intensified warming and, in the WP, decrease in salinity, has lead to a reduction in water density in the upper layers, consequently increasing ocean stratification over the upper 200 m (Cravatte et al. 2009). In the MMM the stratification tends to be too strong in the southern hemisphere, possibly attributable to the tendency for the SPCZ to extend too far east (Fig. 5a-c). Under the ITCZ in the north, the MMM does not capture the full strength of the stratification nor is it well represented in the regions of the cold tongue bias.

Stratification is projected to continue to increase across most of the tropical Pacific (Fig. 5d), with the largest increases occurring in a wide area around the WP and under the SPCZ and ITCZ where both temperature and salinity effects reinforce each other. This increase in stratification is projected to occur at depths of between 20 and 150 m in the WP and at $20-100$ m in PEQD depending on location (thin lines on Fig.4; see also Online Figure S3). In the SPSG and ARCH, the depth range of increase widen to between 30 and 450 m, while increases in the NPTG occur predominantly between the surface and 250 m (Fig.4c; Online Figure S4).

The observed annual maximum depth of the mixed layer (MMLD) does not generally exceed $100-120$ m in the highly stratified WP (Online Figure S5a), but reaches considerably deeper in the centre of the NPTG and SPSG, where high-salinity waters are cooled during the winter, causing convection and much deeper mixing. The MMLD is projected to shoal in most of the tropical Pacific (Online Figure S5d), with the most pronounced shoaling occurring in the WP ($\sim 10-25$ m), and in the western half of both tropical gyre provinces poleward of $\sim 15°$N/S (> 40 m). Under the SPCZ and ITCZ, where model bias is highest (Online Figure S5c), projections are not consistent. Projected increases in the winds near $25°$S / $120°$W will result in the MMLD increasing by up to 40 m in this region.

3.4 Ocean currents and upwelling

Currents within the upper water column are expected to change across the tropical Pacific in the future, particularly as a result of weakened equatorial and north-easterly trade winds and strengthened south easterly trade winds (Bell et al. 2011; Sen Gupta et al 2012b, chapt 3). The MMM projections for large-scale surface currents (0-50 m, Fig. 6b) show relatively small absolute changes away from the equatorial band ($12°$S$-10°$N). Near $9°$S the upper South Equatorial Counter-Current (SECC), which flows eastward across the Pacific, is projected to decrease substantially. Its surface flow is projected to turn towards the south, thereby reducing its penetration to the east. The South Equatorial Current (SEC), which flows westward across the Pacific, is projected to decrease in strength dramatically within $3°$ of the equator, from ~ 30 cm.s^{-1} to ~ 20 cm.s^{-1} in 2100. Just underneath, the upper part of the eastward

flowing Equatorial Under-Current (EUC) is projected to increase substantially, leading to a $\sim$ 20 m shoaling of the EUC core (Fig. 6c). At $\sim$ 7°N, a decrease in the upper part of the eastward flowing North Equatorial Counter-Current (NECC) is projected, while the broad North Equatorial Current (NEC) demonstrates no significant changes. The location of the fronts that lie between the westward equatorial SEC, the eastward SECC and NECC, which define the poleward boundaries of PEQD (Fig. 6b), also demonstrates little projected change.

Upwelling at the equator is projected to decrease in intensity, as are the neighboring two regions of downwelling near 4°N/S (Figure 7). This results in little projected change in the net upwelling integrated between 9°S and 9°N, which is most important to equatorial temperature variations (Zhang and McPhaden 2006).

3.5 Interannual variability

We have explicitly attempted to isolate the global warming signal and remove the effects of year to year variability in our analyses. However, long-term trends are likely to impact ENSO characteristics. At present, there is little consistency across the models with regard to possible changes in the magnitude or frequency of ENSO variability. This is in part related to the significant biases in the climate models and their representation of ENSO (Brown et al this issue). It also relates to the fact that the characteristics of ENSO depend upon a number of competing feedbacks that act to alter its amplitude (Collins et al. 2010). Both CMIP3 and preliminary results from CMIP5 models demonstrate both increases and decreases in frequency and amplitude of ENSO, generally within 20% of their 20th century values (Fig. 2c).

Observations show that the depth of the thermocline decreases during El Niño events and increases during La Niña events in the west Pacific, with the opposite occurring in the east Pacific, on the order of $20-30$ m (Online Figure S6). Average shoaling of the thermocline is projected to be in the order of $\sim 10-20$ m, by 2100. This means that during El Nino events the thermocline could be $\sim$ 40 m shallower than the 20th century mean position in the WP.

As noted above, the mean longitude of the eastern edge of the warm/fresh pool, which is subject to large interannual excursions due to ENSO, will move eastwards in the future. While the projected strength of ENSO (Figure 2c) either increases or decreases depending on the model, projected variability in the location of the fresh pool edge shows either little change or an increased variability (Figure 2b). This highlights non-linearities that are still to be understood in model projections of ENSO.

4 Discussion

4.1 Significance and limitations of this analysis

There are a number of known issues when examining the future projections of the climate of the tropical Pacific. Primary amongst these is the *cold tongue bias*: most of the climate models are too cold along the equator and the cold tongue extends too far to the west. This error also manifests in the simulation of precipitation and ENSO, with impacts on the WP structure. Another major bias is associated with the SPCZ; it is zonally elongated and extends too far to the east in most models (Brown et al 2011). As a result, precipitation and wind patterns are distorted, with consequences for ocean salinity and currents in the southwest Pacific. These biases induce offsets that must be considered when assessing future projections (Brown et al this issue).

Here, we have used output from the full suite of climate models taking part in CMIP3, to examine projections in key physical parameters that are known to affect the distribution of tuna species and their prey. We have also discussed some of the systematic biases that are evident in these properties and examined both historical and projected changes in tropical Pacific over the 21st century. The projections that we report should therefore be interpreted in relation to their location with respect to ecological provinces and dynamical features. For example, as the MMM cold tongue extends too far to the west, we expect that the large warming projected between 140°E and of 160°W may be exaggerated, and a more realistic projection might confine the largest warming to the east of 160°W (Brown et al this issue).

While part of the observational trends discussed herein may be due to natural variability (Vecchi et al 2008), overall agreement with respect to the patterns of change with climate models forced with increasing greenhouse gas concentrations imply that the observed trends are in general consistent with scenarios of anthropogenic Global Warming. By averaging over multiple climate models, we are able to reduce non-systematic model biases and identify regions of model consensus. Averaging, by its nature, removes the effect of outliers. More (or less) extreme projected climate changes are nonetheless feasible. As an example, while the projected MMM SST warming in the warm pool area (defined as the warmest $9.10^6 \mathrm{km}^2$) is 2.7°C, three models show warming that is over 3.2°C.

4.2 Relevance of projections for tuna fisheries

The extension and warming of the WP and associated stratification of the water column is likely to influence tuna distributions and productivity across the tropical Pacific region both directly, through changes in preferred thermal and dissolved oxygen habitats and indirectly, via changing distributions and abundances of tuna forage. Overall, it is anticipated that tuna populations will re-distribute across the tropics and subtropics and overall productivity throughout the region will decrease (Lehodey et al. this issue). However, climate models can show significant inter-model differences in the present day fidelity and their projections of future mean climate and variability and contain a number of significant biases.

Skipjack tuna have a preferred thermal range of 20 to 29°C, with few tuna observed at temperatures beyond $17-30$°C. Along the equator, the boundary of upper preferred temperatures (T= 29°C) is projected to move eastward by 6000 ± 2000 km (Fig.8a), accounting for the large inter-model spread. Below the surface, this isotherm is projected to move down to ~ 100 m west of 170°W, while the depth of the lower preferred temperature (T= 20°C) shows little change. In the eastern part of the basin, the 20°C isotherm is projected to deepen slightly, extending waters of a suitable thermal range to skipjack. In the west Pacific, surface waters warmer than 29°C are projected to expand to 20°S and more than 20°N (Fig.8b, see also Online Figure S7). Assuming similar thermal tolerances into the future and on the basis of preferred thermal habitats alone, skipjack tuna are likely to demonstrate substantial eastward and poleward displacement in their habitat, consistent with existing tuna modeling projections (Lehodey et al. this issue).

The NPTG, SPSG and ARCH provinces are characterized by a thick thermocline and a MMLD which is situated below the euphotic zone Consequently these regions are characterised by low levels of productivity. Projected increases in stratification of the water column in these provinces will increase dynamical barriers, further limiting exchange between the euphotic layer, and the deep, nutrient-rich layer (the *nutricline*), thereby limiting further primary productivity. Conversely, in the WP, the MMLD has little seasonality and is situated within the euphotic zone so that primary productivity can take place beneath it. Projected shoaling of the MMLD may therefore increase nutrient exposure to the sun, leading to enhanced primary production. These processes however, will ultimately depend on the future distribution of nutrients and the position of the nutricline, whose estimation necessitates full biogeochemical models. Recent efforts coupling a biogeochemical model with one of the CMIP3 models projected a deepening in the nutricline, below the WP, resulting in overall lowering of primary production (Bell et al. 2011, chapt. 4).

Most of the models are able to simulate the major current systems in the tropical Pacific. There is however large inter-model differences in the strength and location of the currents. The SECC in particular is poorly represented in many of the models, and non-existent in some of them as a consequence of the SPCZ biases, discussed above. Projected changes in the strength of the major currents across the Pacific will affect biological activities and associated fisheries by influencing horizontal transport of nutrients essential to primary productivity, mixing processes supplying nutrients to the euphotic zone, as well as influencing larval dispersion and connectivity (Munday et al. 2009). The largest projected changes to the upper part $(0-50$ m) of the major currents are those close to the equator where the SECC, NECC and the equatorial part of the SEC are projected to weaken. Sub-surface the upper EUC is projected to shoal substantially and intensify in the western and central Pacific. As the EUC is the primary conduit of iron to the equatorial region (Mackey et al. 2002), such change could increase the productivity in the eastern and central Pacific surface layers, where iron appears to be the limiting nutrient (Sen Gupta et al 2012a).

Dissolved oxygen concentrations are also important in determining future projections of tuna distributions, but are not available in the CMIP3 models. This thereby limits the ability to examine interactions between temperature and oxygen concentrations which may influence future tuna habitats.

5 Conclusions

A number of robust physical changes are projected for the tropical Pacific which are likely to influence tuna distribution and associated fisheries. While there are significant biases in surface temperature in the models which may affect the future distribution of temperature change, substantial warming is evident everywhere, except in the south eastern basin. This places much of the western tropical Pacific outside of the temperature range at which skipjack tuna exist today, reducing dramatically their preferred habitat at low latitudes, and also increasing waters within their thermal range at higher latitudes.

While we find some robust changes in the mean-state, tuna distributions are also subject to dramatic interannual variability and therefore likely to be very sen-

sitive to any future changes in ENSO. Significant biases exist in the simulation of ENSO in the CMIP3 models and there is little consistency with regards to what these models suggest might happen to ENSO characteristics in the future. Considerable work has gone into improving the simulation of ENSO in the new CMIP5 models. Nevertheless, based on our preliminary results from a subset of these models we are still no closer to obtaining a model consensus.

Future warming will be more intense in the surface ocean layers and, along with significant freshening driven by increased rainfall in the west, will lead to an increase in stratification. Increased stratification and weaker winds in the equatorial region is projected to cause a shoaling of the mixed layed in most areas except the southeastern Pacific. This will likely impact both primary productivity and associated tuna forage: In the subtropics, nutrient availability is likely to be reduced. Under the WP, uncertainty in the future depth of the nutricline and associated specific processes make projections of productivity unclear. In the PEQD, the EUC shoaling has a potential to increase productivity; however the combined effect of increases in stratification and reduction in upwelling are not clear.

A number of models participating in CMIP5, will include biogeochemical processes. This will allow direct projections for both physical parameters and nutrient concentrations, oxygen and phytoplankton. Assessing the fidelity of these biogeochemical parameters will be a challenge, however, given the relative sparsity of chemical and biological data compared to physical data such as temperature. This highlights the urgency of initiating and maintaining new continuous monitoring programs, particularly in the South Pacific where there are no long term biogeochemical monitoring programs

Acknowledgements Most of the analyses were based on the international modeling groups participating in IPCC AR4 and AR5, the Program for Climate Model Diagnosis and intercomparison (PCMDI). The IPCC Data Archive: allowed efficient analysis of the massive numerical model outputs. Much of the work described in this paper was commissioned by the Secretariat of the Pacific Community to help assess the vulnerability of fisheries and aquaculture in the tropical Pacific to climate change. J. Lefèvre's technical help was most valuable. We thank Johann Bell for his guidance on how to present the analyses to make them easy for fisheries scientists to use. K. Richard and N. Holbrook also provided valuable feedback at early stages of this work.

References

Bell J, Johnson J, Hobday A (2011) Vulnerability of Tropical Pacific Fisheries and Aquaculture to Climate Change, secretariat of the pacific community edn. Bell, J., Johnson, J. and Hobday A., Noumea, New Caledonia. 927pp.

Brown JR, Power SB, Delage FP, Colman RA, Moise AF, Murphy BF (2011) Evaluation of the south pacific convergence zone in IPCC AR4 climate model simulations of the twentieth century. Journal of Climate 24(6):1565–1582.

Brown JN, Sen Gupta A, Brown JR, Muir LC, Risbey JS, Zhang X, Ganachaud A, Murphy BF, Wijffels S (2012) Implications of CMIP3 model biases and uncertainties for climate projections in the western tropical pacific. Climatic Change, this issue.

Bushnell PG, Brill RW (1992) Oxygen transport and cardiovascular responses in skipjack tuna (Katsuwonus pelamis) and yellowfin tuna (Thunnus albacares) exposed to acute hypoxia. J. of Comp. Physiol B 162(2):131–143

Collins M, An SI, Cai WJ, Ganachaud A, Guilyardi E, et al. (2010) The impact of global warming on the tropical pacific ocean and El Niño. Nature Geoscience 3(6):391–397

Cravatte S, Delcroix T, Zhang D, McPhaden M, Leloup J (2009) Observed freshening and warming of the western pacific warm pool. Climate Dynamics 33(4):565–589

DiNezio PN, Clement AC, Vecchi GA, Soden BJ, Kirtman BP, Lee S (2009) Climate response of the equatorial pacific to global warming. J. of Climate 22:4873–4892,

Durack PJ, Wijffels SE (2010) Fifty-year trends in global ocean salinities and their relationship to broad-scale warming. J. of Climate 23(16):4342–4362, DOI 10.1175/2010JCLI3377.1,

Han W, Meehl GA, Hu A (2006) Interpretation of tropical thermocline cooling in the indian and pacific oceans during recent decades. Geophysical Research Letters 33(23), DOI 10.1029/2006GL027982,

Johnson G, Wijffels S (2011) Ocean density change contributions to sea level rise. Oceanography 24(2):112–121,

Lehodey P, Bertignac M, Hampton J, Lewis A, Picaut J (1997) El Niño Southern Oscillation and tuna in the western pacific. Nature 389(6652):715–718.

Lehodey P, Senina I, Calmettes B, Hampton J, Nicol J (2012) Modelling the impact of climate change on pacific skipjack tuna population and fisheries. Climatic Change, this issue.

Longhurst AR (2006) Ecological geography of the Sea. Academic Press, New York, USA.

Mackey D, O'sullivan J, Watson R (2002) Iron in the western pacific: a riverine or hydrothermal source for iron in the equatorial undercurrent? Deep Sea Res. Part I, 49(5):877–893.

Maes C, Picaut J, Kuroda Y, Ando K (2004) Characteristics of the convergence zone at the eastern edge of the pacific warm pool. Geophysical Research Letters 31(11), DOI 10.1029/2004GL019867.

Munday PL, Leis JM, Lough JM, Paris CB, Kingsford MJ, Berumen ML, Lambrechts J (2009) Climate change and coral reef connectivity. Coral Reefs 28:379–395

Nakicenovic NJ, Alcamo J, Davis G (2000) IPCC special report on emissions scenarios (SRES). Tech. rep., Cambridge University Press

Pennell C, Reichler T (2011) On the Effective Number of Climate Models, J. of Climate, 24(9), 2358-2367.

Sen Gupta A, Santoso A, Taschetto AS, Ummenhofer CC, Trevena J, England MH (2009) Projected changes to the southern hemisphere ocean and sea ice in the IPCC AR4 climate models. J. of Climate 22(11):3047–3078.

Sen Gupta A, Ganachaud A, McGregor S, Brown JN, Muir LC (2012a) Drivers of the projected changes to the pacific ocean equatorial circulation. Geophys Res Lett 39(9) DOI 10.1029/2012GL051447.

Sen Gupta A, Muir LC, Brown JN, Phipps SJ, Durack PJ, Monselesan D, Wijffels SE (2012b) Climate drift in the CMIP3 models. Journal of Climate 25(13):4621–4640.

Tebaldi C, Knutti R (2007) The use of the multi-model ensemble in probabilistic climate projections. Proc. R. Soc. A: Mathematical, Physical and Engineering Sciences 365(1857):2053–2075.

Vecchi GA, Clement A, Soden BJ (2008) Examining the tropical pacific's response to global warming. Eos, Transactions American Geophysical Union 89(9):81.

Xie S, Deser C, Vecchi GA, Ma J, Teng H, Wittenberg AT (2010) Global warming pattern formation: Sea surface temperature and rainfall. J. of Climate 23:966–986.

Zhang D, McPhaden MJ (2006) Decadal variability of the shallow pacific meridional overturning circulation: Relation to tropical sea surface temperatures in observations and climate change models. Ocean Model. 15(3-4):250–273.

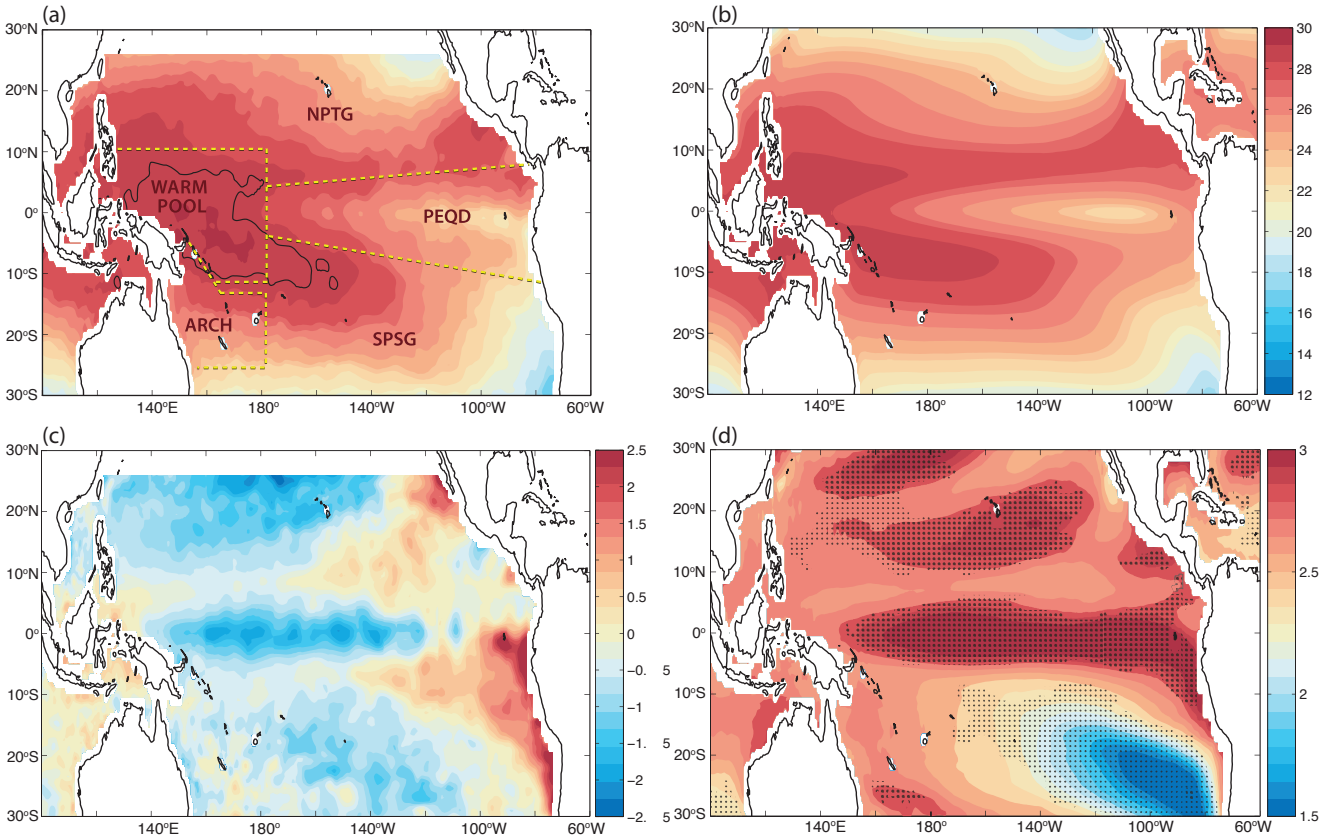

Fig. 1 (a) Observed climatological SST from CARS with warm pool boundary (contour at 29°C) and oceanic provinces superimposed, (b) multi-model mean (MMM; 1980-1999) SST, based on 19 models, (c) MMM bias compared to observations, with a strong cold bias along the equator (d) change in SST per 100 years for 21st century of the simulation under the SRES A2 scenario (based on a linear trend line). Quantitative model agreement is ubiquitous at 95% based on a Student t-test; Mottling indicates regions where there is at least 80% agreement on the sign of the temperature change when the area mean change has been removed (i.e. a measure of the agreement in the spatial pattern of change). Oceanic provinces are as follows: Pacific Equatorial divergence (PEQD), Pacific Warm Pool (WP), North Pacific Tropical Gyre (NPTG), South Pacific Subtropical Gyre (SPSG) and the Archipelagic Deep Basins (ARCH).

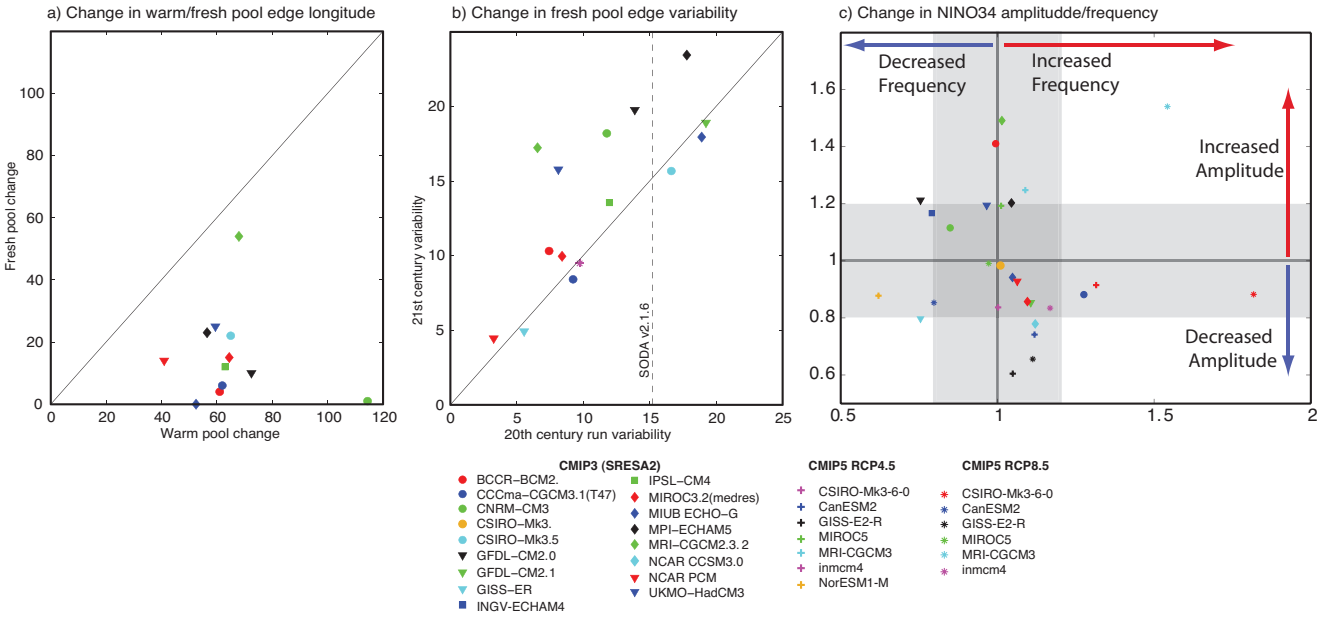

Fig. 2 Changes in WP and ENSO variability. a) change in the longitude of the equatorial (3°S to 3°N) warm pool and fresh pool edge over the 21st century in individual CMIP3 models. b) change in the variability of the fresh pool edge (°longitude, 1 standard deviation). The fresh pool and warm pool are defined by model specific isohalines and isotherms, respectively, chosen such that the area of bounded freshwater or warm water was equivalent to the area contained within the T= 29°C isotherm and S= 34.8 isohalines in the observations from CARS. c) Ratio of 2050-2100 to 1950-2000 frequency and amplitude of temperature anomalies (NINO3.4 index). Amplitude corresponds to one standard deviation. Frequency was computed as a weighted average of NINO3.4 frequency by spectral power for all frequencies whose power was significant at 95% level. Panels (b) and (c) contain addition preliminary results from the CMIP5 archive. CMIP5 data is still in progress and modelling groups may replace certain data in the future. The shaded area delimits the 20% change.

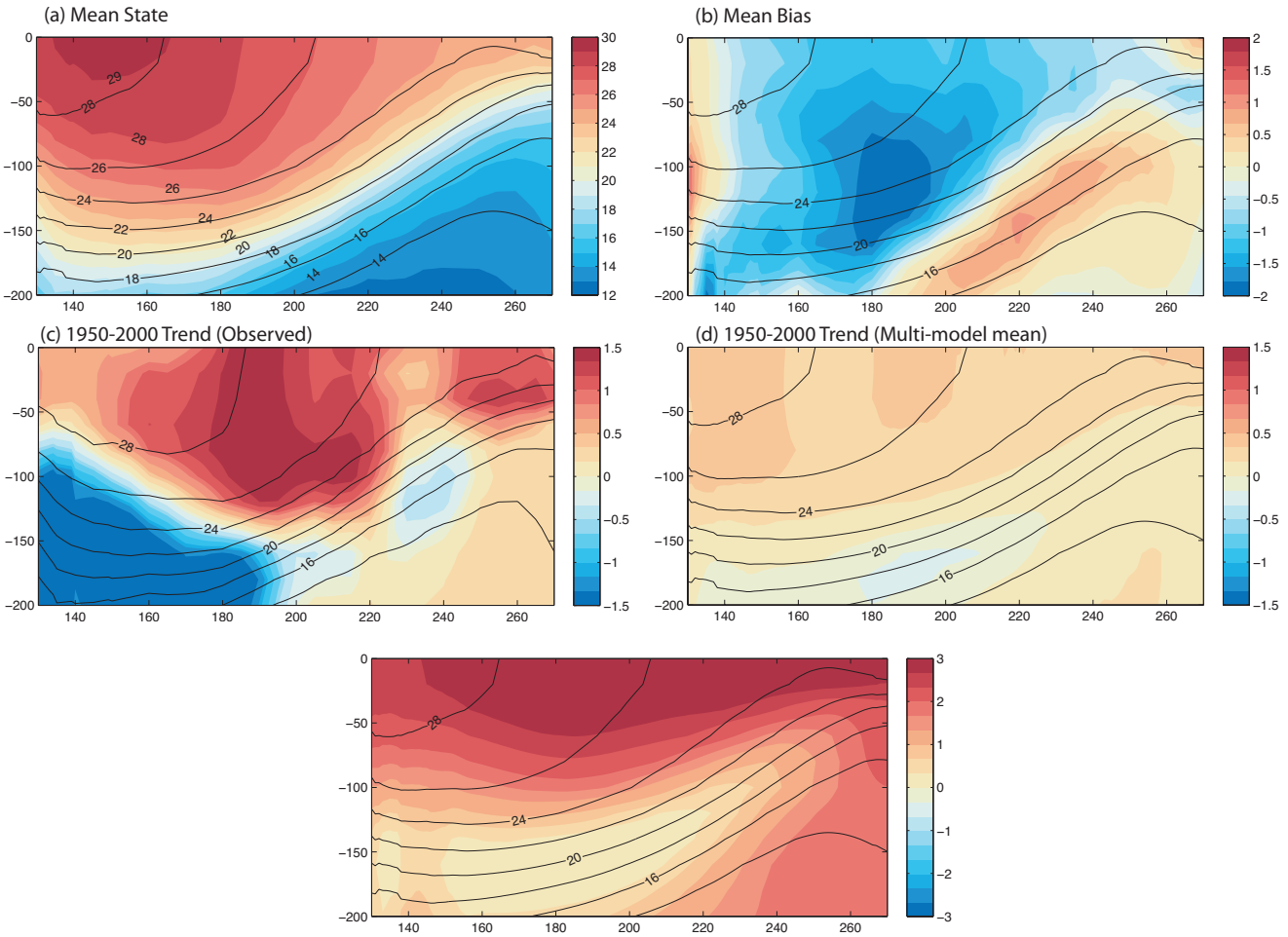

Fig. 3 Equatorial potential temperature averaged 5°S to 5°N (°C) as a function of longitude and depth. a) Observed long-term mean b) Model bias (MMM− observations). c) Observed linear temperature trend over 50 years. d) MMM trend over 1950-2000. e) Projected trend in temperatures 2000-2100 (color shading). Overlaid (line contours) is the MMM 1950-2000 mean (a,b,d,e) and observed long-term mean (c). Observations are based on a new dataset (Durack and Wijffels 2010; Johnson and Wijffels 2011) that has used observations from 1950-2008 to compute the mean state and trends (expressed as a 1950-2000 trend). Multi-parametric regression technique was employed to reduce aliasing of the trend by various modes of climate variability including ENSO and the PDO.

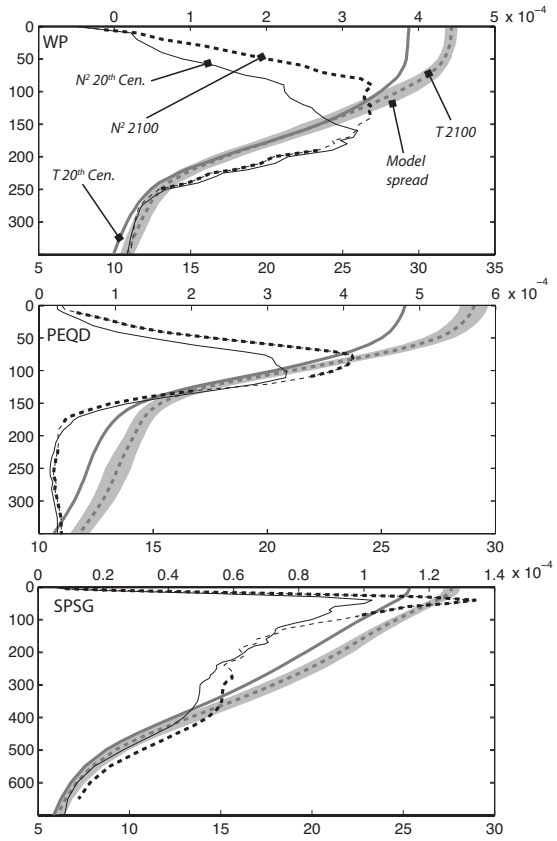

Fig. 4 Average vertical temperature profiles for typical sites of each province (°C). The thick grey line corresponds to the modern climatological temperature from CARS; the grey dashed line corresponds to projected MMM 100-year trend added to CARS (1 standard deviation model spread: shaded region). The MMM stratification, thin black lines, is indicated by Brunt-Väisälä frequencies, N^2 (i.e the measure of the strength of the vertical density gradient). Projected N^2, dashed black line, is thickened where the change is significant at 95% level. Provinces are defined as follows a) WP 5°S−5°N / 155°E−160°E; b) PEQD 3°S−3°S / 140°W−130°W; c) SPSG 25°S−20°S 160°W−140°W.

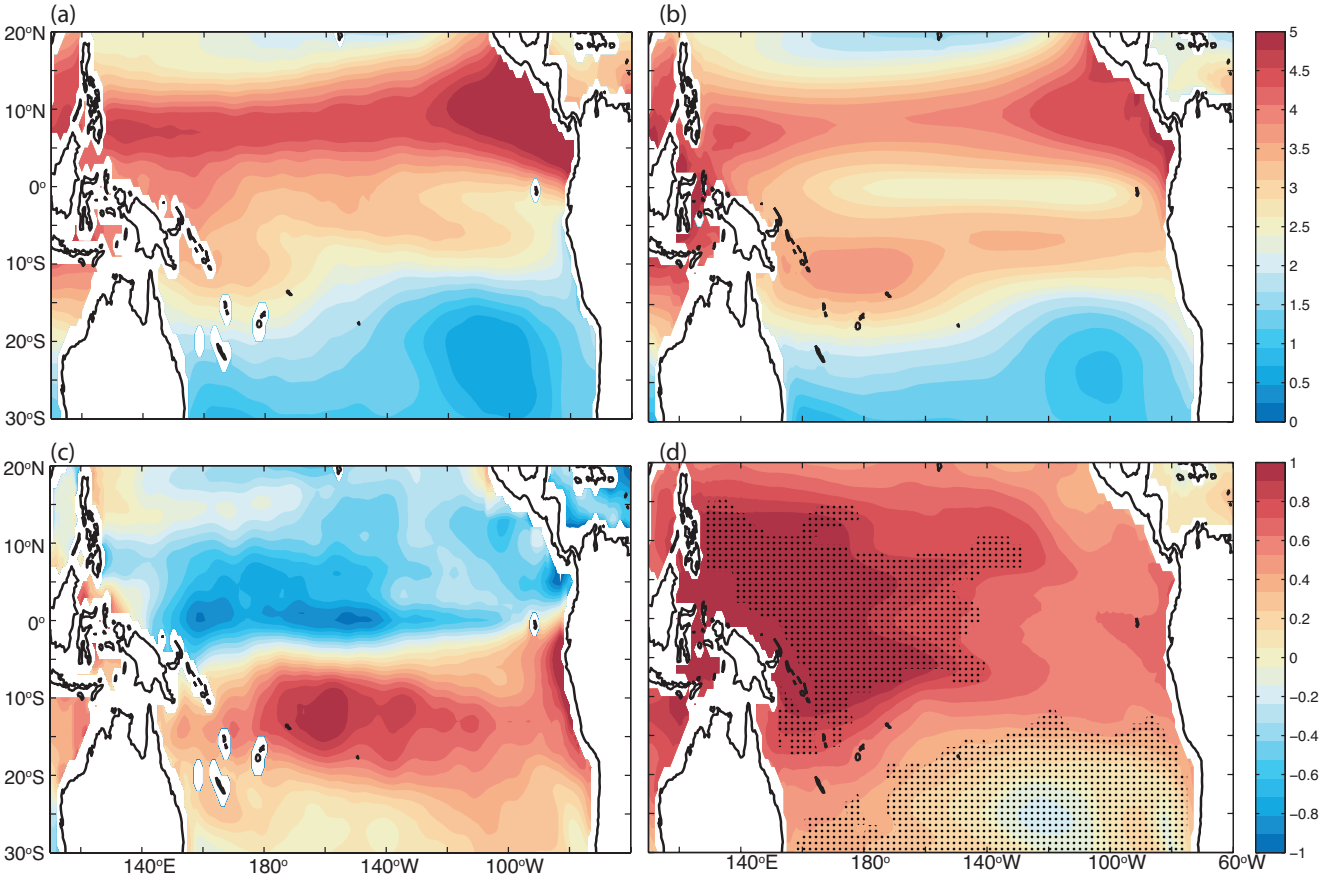

Fig. 5 Same as Fig. 1 but for density difference between 200m and surface (kg.m^{-3}) (a) observed (WOA09), (b) MMM, (c) MMM bias, (d) MMM projected change over the 21st century for A2 scenario. Mottling indicates regions where there is at least 80% agreement on the sign of the change when the area mean change has been removed (i.e. a measure of the agreement in the spatial pattern of change).

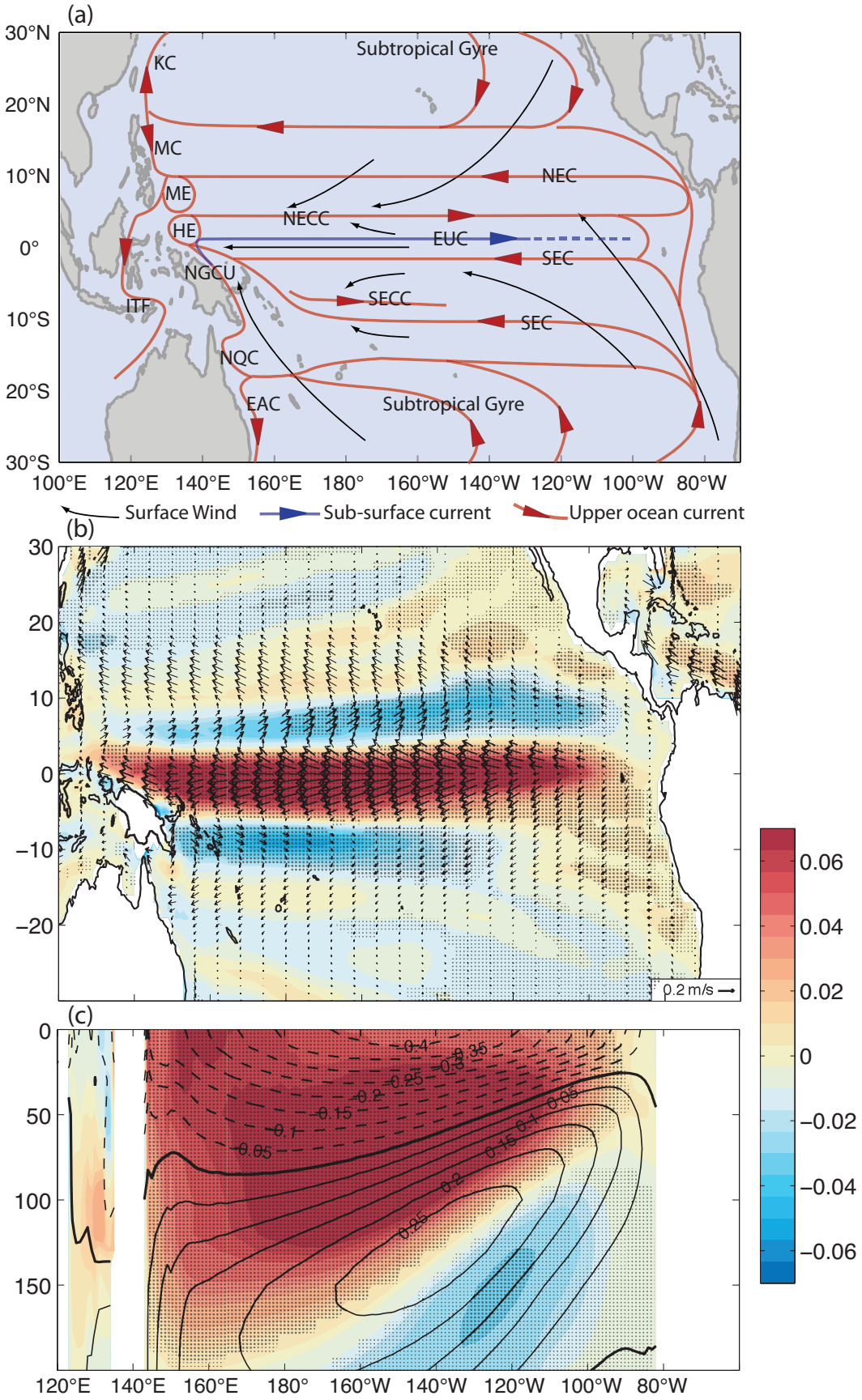

Fig. 6 a) The primary ocean currents in the upper 100 to 200 m: In the subtropical gyre, two broad flows carry water westward: the North Equatorial Current (NEC) and the South Equatorial Current (SEC). At the equator, a strong Equatorial Undercurrent (EUC) carries waters to the east below the SEC. Narrow vigorous currents occur at the western boundaries: East Australian Current (EAC); North Queensland Current (NQC); New Guinea Coastal Current (NGCU); Halmahera Eddy (HE); Mindanao Eddy (ME); Mindanao Current (MC); and Kuroshio Current (KC). Some of the water outflows toward the Indian Ocean (Indonesian Throughflow, ITF). Below atmospheric convergence zones, counter-current appear near the surface and above the NEC and SEC: the North Equatorial Countercurrent (NECC) and the South Equatorial Counter Current (SECC). b) Mean state (arrows) and projected change (colour contours) to the surface (0-50 m) zonal circulation; c) as (a) for equatorial zonal flow averaged between 3°S and 3°N. Full line contours represent mean westward flow, contour interval 5 cm.s^{-1}. Mottling shows where the change is signicant at 95% using a Student t-test.

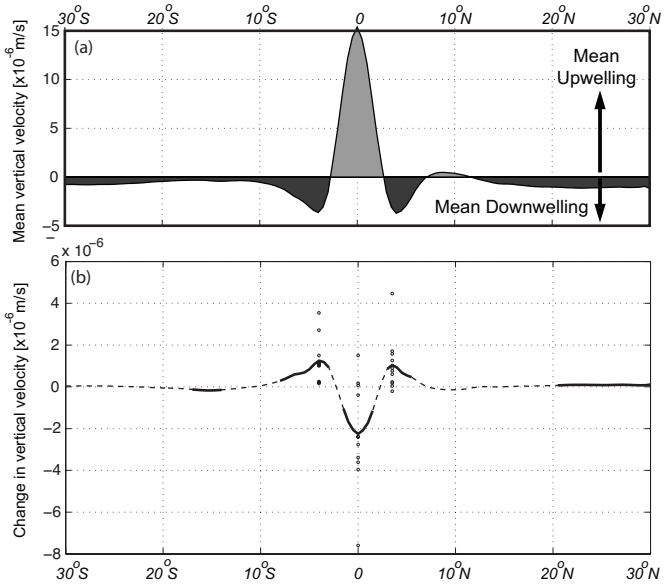

Fig. 7 a) Vertical velocities of water (10^{-6} m.s^{-1}) at a depth of 50 m, for 1990 (mean 1980 − 1999), averaged between 170°E and 110°W, where a positive velocity corresponds to upwelling and a negative velocity to downwelling; and b) Climate driven changes to vertical velocities for 2100 (full line if significant at 95%; dashed line otherwise). Values for individual CMIP3 models are indicated in the maxima (small circles). The strong equatorial upwelling shows decreases that are immediately balanced by strong downwelling near 4°N−4°S so that net upwelling between 9°S and 9°N does not change.

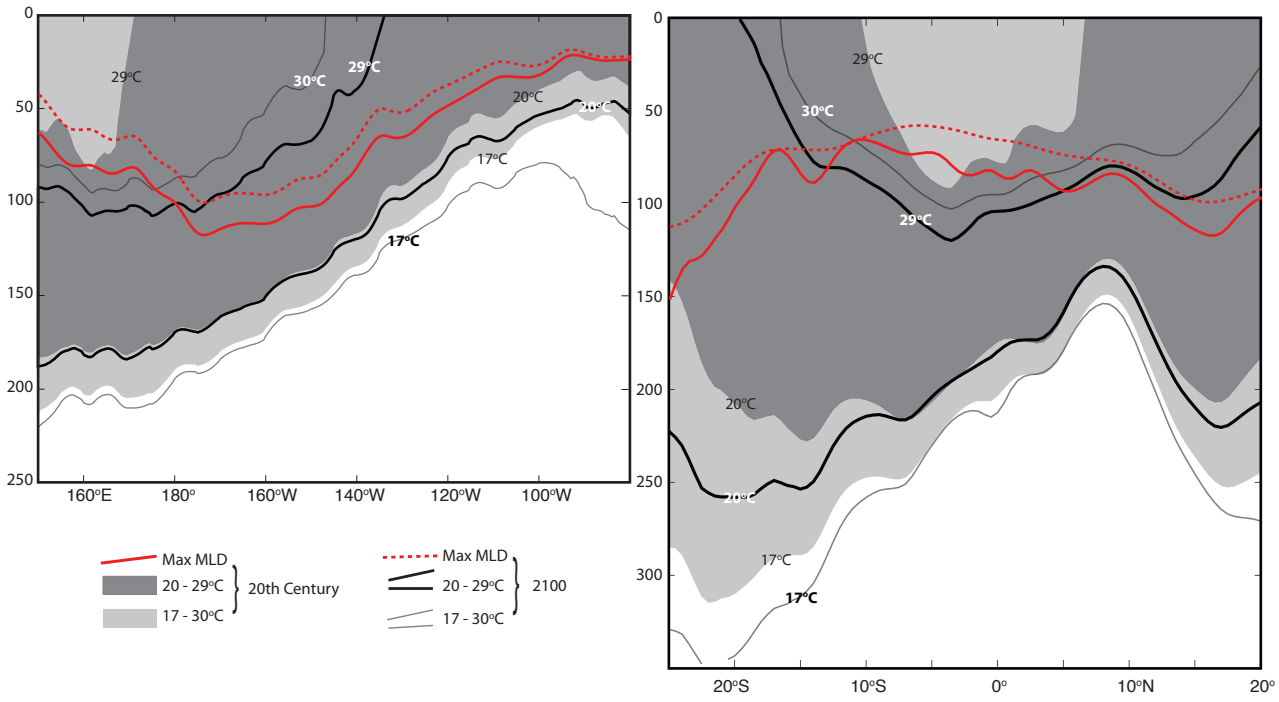

Fig. 8 a) Isotherm depths: present day and projected along the equator (3°S to 3°N). 20° − 29°C is the normal range for skipjack tuna; 17° − 30°C are the extreme ranges. b) Same but for longitudes 165°E. Data has been bias corrected, i.e. present day is observed distribution and projections are observed distribution plus anomalies from the climate models.